Generating Quasi-Single-Cycle Relativistic Laser Pulses by Laser-Foil Interaction

L. L. Ji (吉亮亮),[1] B. F. Shen (沈百飞),[1,*] X. M. Zhang (张晓梅),[1] F. C. Wang (王凤超),[1] Z. Y. Jin (金张英),[1] C. Q. Xia (夏长权),[1] M. Wen (温猛),[1] W. P. Wang (王文鹏),[1] J. C. Xu (徐建彩),[1] and M. Y. Yu (郁明阳)[2,3]

[1]*State Key Laboratory of High Field Laser Physics, Shanghai Institute of Optics and Fine Mechanics, Chinese Academy of Sciences, Post Office Box 800-211, Shanghai 201800, China*

[2]*Institute for Fusion Theory and Simulation, Zhejiang University, Hangzhou 310027, China*

[3]*Institut für Theoretische Physik I, Ruhr-Universität Bochum, D-44780 Bochum, Germany*

(Received 6 June 2009; published 19 November 2009)

A scheme for producing nearly single-cycle relativistic laser pulses is proposed. When a laser pulse interacts with an overdense thin foil, because of self-consistent nonlinear modulation, the latter will be more transparent to the more intense part of the laser, so that a transmitted pulse can be much shorter than the incident pulse. Using two-dimensional particle-in-cell simulation and analytical modeling, it is found that a transmitted pulse of duration 4 fs and peak intensity 3×10^{20} W/cm^2 can be generated from a circularly polarized laser pulse. The intensity of the resulting pulse is only limited by that of the incident pulse, since this scheme involves only laser-plasma interaction.

DOI: 10.1103/PhysRevLett.103.215005 PACS numbers: 52.38.−r, 42.65.Re, 52.27.Ny, 52.65.Rr

Recent significant improvements of laser-light contrast by means of the double plasma mirror [1] and other techniques [2] allows an intense laser pulse to interact with a solid-density foil before the latter is damaged by the prepulse of the laser. Very hard diamondlike foils of ultrasmall, say 4.5 nm, thickness comparing with the skin depth of the light are now available. An important application of such thin foils is for ion acceleration by laser interaction with dense plasmas, such as that of foil normal sheath acceleration [3–6], shock acceleration [7–9], direct laser-pressure acceleration [10–12], and other methods [13–15]. The most efficient method, namely, by direct laser-pressure acceleration, requires high-contrast laser pulse as well as foil targets of nanometer thickness. Another application is to use an ultrathin foil as a relativistic mirror for generating high-intensity ultrabright x- and γ-ray radiation by relativistic Doppler shifting the light [16]. Laser energy can also be trapped and accumulated to very high levels between two closely placed ultrathin foils when two oppositely directed ultraintense laser pulses impinge on them [17].

Nearly single-cycle lasers are suitable for generating single attosecond pulses [18] as well as for electron acceleration in the small bubble regime [19,20]. Several methods for obtaining single-cycle laser pulses have been proposed, most of which are optical [21]. However, owing to the relatively low damage threshold of the optical components and other problems, the intensity of the optically produced single- and few-cycle laser pulses is very limited. In this Letter, it is shown by analytical modeling and PIC simulation that one can produce few-fs nearly single-cycle ultraintense light pulses from laser interaction with ultrathin foils. When laser light interacts with an adequately thin overdense plasma, both are self-consistently (nonlinearly) modulated. For suitably chosen laser and foil parameters, the foil is transparent only to the highest-intensity part of the laser pulse. As a result, the transmitted light pulse has a much shorter duration than the incident-pulse, as shown in Fig. 1. The pulse duration depends primarily on the laser-light intensity gradient and foil conditions. Since the process involves only laser-plasma interaction, like the plasma grating [22], there should be no intensity limitation due to material damage.

We shall firstly perform a one-dimensional (1D) particle-in-cell (PIC) simulation with LPIC++ [23]. The normalized amplitude $\mathbf{a} = e\mathbf{E}_0/m_e\omega_0 c$, where e and m_e are the electronic charge and mass, respectively, $\mathbf{E}_0$ is the laser electric field, ω_0 is the laser frequency, and c is the speed of light, of the circularly polarized (CP) incident laser pulse, propagating in the x direction, is given by $\mathbf{a} = a_m \sin^2(\pi t/2\tau)[\sin(\omega_0 t)\hat{\mathbf{e}}_y + \cos(\omega_0 t)\hat{\mathbf{e}}_z]$, where $a_m = 20$ is the peak amplitude and $\tau = 4$ is the pulse duration normalized by the laser period T_0. The laser light is of wavelength $\lambda_0 = 1$ μm. The simulation box is $50\lambda_0$ in the x direction, and the foil is initially located between

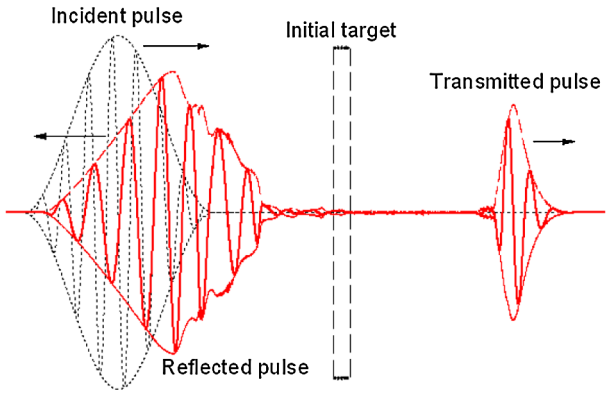

FIG. 1 (color online). Scheme for generating a near-single-cycle laser pulse. The incident pulse interacts with a thin foil target, producing an ultrashort transmitted pulse and a reflected pulse.

$x = 20\lambda_0$ and $20.7\lambda_0$. The normalized (by the critical density $n_c = m_e\omega_0^2/4\pi e^2$) foil density is $N_0 = 8$. The cold foil plasma is taken to be fully ionized and the ion-to-electron mass ratio is $m_i/m_e = 1836$. The simulation mesh size is $\lambda_0/200$.

Figure 2(a) shows the trajectories of 71 electrons and 71 protons that are initially uniformly distributed in the foil. The laser field immediately behind the foil is also shown. The incident pulse arrives at the foil at $t = 20T_0$, and its rising part pushes the foil electrons inward. An electron layer is formed and compressed by the laser ponderomotive force. Laser-light transmission through the foil occurs at about $t = 23T_0$. As the electron layer is further compressed, the transmitted laser field increases rapidly and reaches a maximum at about $t = 25T_0$, when the compression is also maximal. When the trailing part of the incident pulse enters the foil plasma, the foil protons start to move forward with the electron layer because of the space charge field. The transmitted field also drops sharply from its peak value, resulting in an ultrashort, nearly single cycled transmitted light pulse with duration $1.1T_0$ and peak amplitude $a = 12.5$. That is, at the cost of (still acceptable) amplitude reduction (from 20 to 12.5), the duration of the incident pulse is narrowed to about one fourth of the incident pulse. One can also see that as the peak of the incident pulse enters the plasma, ion motion becomes significant. This can be attributed to the fact that at this stage, the charge-separation field has become sufficiently strong. The electrons and ions are then driven forward by the laser as a double layer. The spectrums of incident and transmitted laser pulses are shown in Fig. 2(b). One can see that the light spectrum is broadened by about 3 times because of the pulse shorting. The central frequency is barely changed, showing that there is almost no frequency shift and the number of light-wave cycles is indeed reduced by the pulse shortening.

We now consider in more detail the physics of the pulse compression process. Figure 3(a) shows a model of the laser-foil interaction process [24]. In the model, the electron dynamics in the laser-foil interaction is treated as quasistatic in the sense that as the laser field varies with time, for each value of a, the corresponding stationary solution is obtained. This approximation is valid for overdense ($N_0 = 8$) plasmas, since the plasma response time $\omega_{pe}^{-1} \sim T_0/N_0^{1/2}$ is much smaller than pulse duration $\tau(= 4T_0)$. In this model, the ions remain stationary.

The normalized vector potential of laser field at $\xi = \omega_0 x/c$ can be written as $a = a_0(\xi)\exp[i\omega_0 t + i\theta(\xi)]$, where $\theta(\xi)$ is the wave phase. Two constants of motion of an electron moving in the laser field are [25]

$$M = (\gamma^2 - 1)\partial_\xi\theta, \tag{1}$$

$$W = [(\partial_\xi\gamma)^2 + M^2]/2(\gamma^2 - 1) + \gamma^2/2 - N_0, \tag{2}$$

where $\gamma = (1 + a^2)^{1/2}$ is the relativistic factor for the CP laser pulse. Requirement of stationary solutions gives [23]

$$\partial_\xi\gamma = \partial_\xi\psi \equiv -E_x, \tag{3}$$

where $\psi = e\phi/m_e c^2$ is the normalized scalar potential and $E_x = -\partial_x\phi$ is the electrostatic charge-separation field. Invoking continuity of the transverse electric and magnetic fields at the interfaces ξ_b and ξ_c, we have

$$a_4^2 = a_c^2 = M, \qquad \partial_\xi a_4 = 0, \quad \text{and} \quad W = |M| + 1/2 - N_0(1 + |M|)^{1/2}, \tag{4}$$

$$(\partial_\xi a_b)^2 + M^2/a_b^2 + a_b^2 = 4a_1^2 - 2M, \tag{5}$$

$$[(\partial_\xi\gamma_b)^2 + M]/2(\gamma_b^2 - 1) + \gamma_b^2/2 - N_0\gamma_b = W. \tag{6}$$

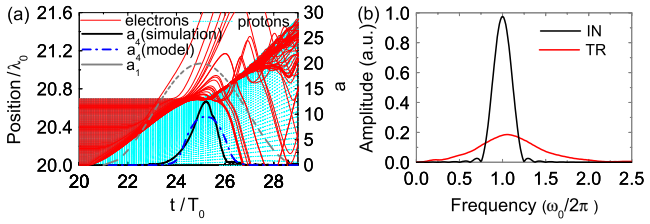

FIG. 2 (color online). PIC simulation results for $a_m = 20$, $\tau = 4$, and $d = 0.7$ (normalized by laser wavelength). (a) Electron and proton trajectories, and the laser field a_4 at the foil backside from simulation and analytical model, as well as the incident laser field a_1. (b) Spectrums of the incident (IN) and the ultrashort transmitted (TR) light pulses.

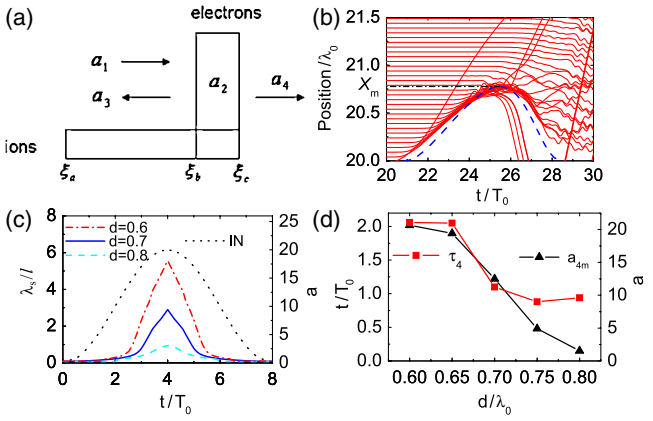

FIG. 3 (color online). (a) The laser-foil interaction model. The incident, reflected, transmitting, and transmitted laser fields are denoted by a_1, a_2, a_3, and a_4, respectively. The initial left and right surfaces of the foil are at ξ_a and ξ_c. The interface of the laser front and the electron layer is at ξ_b. (b) Electron trajectories (solid line) from 1D PIC simulations for immobile ions and the calculated interface position $\xi_{ba} = \xi_b - \xi_a$ (dashed line) versus time for $a_m = 20$, $\tau = 4$, $N_0 = 8$, and $d = 4$. The maximum displacement of the interface is marked by X_m. (c) Calculated value of λ_s/l versus time for $d = 0.6$ (dash-dot line), 0.7 (solid line), and 0.8 (dashed line). The pulse shape of the incident laser (dotted line) is also shown. (d) The peak amplitude a_{4m} (triangle) and duration τ_4 (square) of the generated pulse versus target thickness with $a_m = 20$, $\tau = 4$, and $N_0 = 8$ from simulations.

Applying Eqs. (3) to (6) to the configuration in Fig. 3(a), we can obtain a_4 and $\xi_{ba} = \xi_b - \xi_a$, as well as the other physical quantities [24].

In order to compare the results from the analytical model and the PIC simulation, we have simulated the case $d = 4$ keeping the ions immobile, but the other parameters the same as that in Fig. 2. The simulated electron trajectories are shown in Fig. 3(b). Through imbalance of the ponderomotive and the electrostatic charge-separation forces, the electrons are steadily pushed inward as well as reflected, corresponding to the rising and falling regions of the incident pulse. The relative position (ξ_{ba}) of the electron layer versus time calculated from our analytical model is given by the solid line in Fig. 3(b). The two results agree very well.

An important parameter in the scheme is the maximum displacement X_m of the surface of the electron layer. It is associated with the peak laser amplitude, calculated to be $X_m \simeq 0.77\lambda_0$, as seen in Fig. 3(b). This value also agrees with that from the simulation. When the foil is too thick, say $d = 4$, no transmission occurs. If the foil thickness is reduced to about X_m, which is still larger than the skin depth, significant laser-light transmission takes place because of compression of the electron layer. The laser field decays as e^{-x/λ_s} in an overdense plasma, where $\lambda_s = c/\omega_{pe} = (\gamma_b/N_0)^{1/2}(l/d)^{1/2}\lambda_0/2\pi$ is the skin depth. When the electron layer in a foil of thickness d is compressed to thickness l, the parameter $\alpha = \lambda_s/l \sim 1/\ln(E_0/E_t)$ can be used to represent the foil transparency. Accordingly, we have

$$\alpha = \frac{\lambda_0}{2\pi}\left(\frac{\gamma_b}{N_0}\frac{1}{d}\right)^{1/2}\frac{1}{l^{1/2}}, \tag{9}$$

so that if the skin depth is larger than the layer thickness, i.e., $\alpha > 1$, laser transmission would be significant. No transmission can occur if $\alpha \ll 1$. To see how the transparency is related to the laser amplitude, we have calculated α versus time for three different initial foil thicknesses around X_m. It can be clearly seen in Fig. 3(c) that for all the three thicknesses, α firstly increases with rising laser amplitude, reaches a maximum at the peak incident-pulse amplitude, and then decreases with the falling part of the laser pulse. That is, the foil transparency is modulated by laser amplitude: the less intense part of the pulse is reflected and the more intense part can easily pass through. As a result, the transmitted light pulse is much shorter than the incident pulse, and an ultrashort laser pulse is produced. Figure 3(c) also shows the effect of the foil thickness. In the case $d = 0.8$, since the peak value of α is rather small (~ 1), the transmitted pulse is of low intensity. A thinner foil such as $d = 0.6$ yields larger peak transparency, but the duration of the resulting pulse is also longer. The case $d = 0.7$ presented in Fig. 2 offers both short duration and large amplitude. Figure 3(d) shows the relationship between parameters of the transmitted pulse and target thickness. One can choose appropriate target thickness for specific application requirements. We should notice that with increasing target thickness, the peak amplitude of the transmitted pulse decreases all along while its duration decreases rapidly to about one cycle at $d = 0.7$ and becomes saturated. It means that $d = 0.7$ corresponds to a pulse with largest peak amplitude in nearly single-cycle region, which is consistent with the analysis in Fig. 3(c).

The temporal profiles of the generated laser pulse from the simulation and the analytical model for $d = 0.7$ are also compared in Fig. 2(a). We see that the agreement is quite good. A difference is that the ultrashort pulse from the simulation is not symmetrical, with the tail part steeper than the rising front. This can be attributed to ion motion. As mentioned, when most of the incident pulse has entered the target, the ions and electrons are driven forward as a double layer. If the latter has a velocity v, the light, or ponderomotive, pressure P_L on it can be written as [11]

$$P_L = \frac{E_0^2}{2\pi}\frac{c - v}{c + v}, \tag{10}$$

where the Doppler effect has been included. From Eq. (10), we see that the induced velocity v reduces the light pressure by a factor $(c - v)/(c + v)$ and thus weakens the compression of the layer. The layer thickness l would then be larger than that in the immobile-ion case of the analytical model. From Eq. (9), we have $\lambda_s/l \sim l^{-1/2}$ so that the foil transparency decreases with increasing l, leading to a shortened pulse tail, even if the incident pulse has a longer tail. In present simulation, the layer velocity is about $v/c \sim 0.2$ as the peak laser field interacts with the foil, which decreases the light pressure by nearly 50% according to Eq. (10).

Some electrons at the foil backside are driven away by the lightwave electric field of the transmitted pulse directly, which has not been included in our analytical model; therefore, the transparency of the target (hence, the peak amplitude of transmitted pulse) in simulation is somewhat higher, as can be seen in Fig. 2(a).

The gradient of the incident-pulse profile ($\sim a_m/\tau$) is a key factor affecting the properties of the transmitted pulse. It determines the variation of the transparency of the plasma layer during the laser-plasma interaction. The electron trajectories in Fig. 2(a) suggest that if the incident pulse rises more gently, the value of α governing the foil transparency would then vary more slowly (as in the case of a shorter incident pulse), resulting in a longer transmitted pulse. For example, with $a_m = 10$, $\tau = 4$, and $N_0 = 8$, where the amplitude gradient is halved and $X_m \simeq 0.38\lambda_0$, one generates a transmitted pulse of $a_{4m} \simeq 6$ and $\tau_4 \simeq 1.5$ with $d = 0.35$. The duration is apparently larger than in Fig. 2(a).

It should be mentioned that it is difficult to tell analytically how large the amplitude gradient shall be to gain a

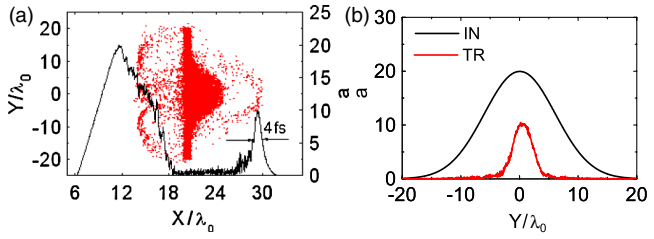

FIG. 4 (color online). Results from 2D PIC simulations. The laser parameters are $a_m = 20$, $\tau = 4$, and the transverse FWHM is $12\lambda_0$. The foil density is $N_0 = 8$, and the thickness is $d = 0.75$. (a) Electron distribution (dots) and axial laser profiles at $Y = 0$ (solid line). (b) Transverse profiles of the incident (IN) and transmitted (TR) laser pulses.

quasi-single-cycle pulse, because the duration is also related to target thickness. However, for each a_m and τ, one can always follow the above process to gain the relationship between transmitted and incident pulses with different target thickness, as seen in Fig. 3(d), and consequently choose the appropriate parameters.

Two-dimensional PIC simulations of the proposed scheme are carried out to see the effect of higher dimensions. The simulation box is $50\lambda_0 \times 50\lambda_0$ in the X and Y directions. The $N_0 = 8$ cold-plasma foil occupies the region $20\lambda_0$ to $20.75\lambda_0$ in the X direction and $-20\lambda_0$ to $20\lambda_0$ in the Y direction. The mesh size is $(\lambda_0/60) \times (\lambda_0/60)$. A CP laser pulse, with $a_m = 20$, $\tau = 4$, and transverse FWHM $12\lambda_0$, illuminates the foil from the left. The foil thickness is slightly increased (comparing to the 1D case) to $d = 0.75$ in order to compensate the foil deformation by hole boring. Figure 4(a) shows the electron distribution and axial laser profiles at $Y = 0$. The transverse profile of the incident and transmitted pulses at the position of the peak intensity in the X direction are shown in Fig. 4(b). We see that in 2D, an ultrashort laser pulse can still be generated. The pulse duration is ~ 4 fs and the peak intensity is $\sim 3 \times 10^{20}$ W/cm^2, comparable to the 1D results (3.7 fs, 4.3×10^{20} W/cm^2). The transverse FWHM of the transmitted pulse, which is determined mainly by the focal spot size of incident pulse, is $\sim 4\lambda_0$. That is, the transmitted pulse is localized in a $1.2\lambda_0 \times 4\lambda_0$ region. Thus, the present scheme offers a possibility for producing a high-intensity λ_0^3 laser pulse [26]. In Fig. 4(a), there are still some breaking away electrons comoving with the transmitted pulse. Their energy is around tens of MeV, thus can be separated from the generated pulse through a one-tesla magnetic field.

In summary, using PIC simulations and analytical modeling, we have shown that a nearly single-cycle relativistic laser pulse can be obtained when a CP laser pulse interacts with a dense foil. The scheme is based on the fact that the transparency of the foil plasma is modulated by the laser such that only a small segment associated with the most intense part of the latter is transmitted, the rest are reflected and absorbed. The results from the simulation and the quasistatic model agree well, and the dependence on the transparency parameter controlling the intensity and width of the transmitted pulse is investigated. The main conclusions are also verified by 2D PIC simulations. Apparently, there is also little limitation on the transmitted-pulse duration, which depends mainly on the gradient of the incident-pulse profile, since one can use multiple foils to obtain consecutively shorter pulse durations. It is of interest to point out that our proposed scheme relies on the use of submicron foils and hence high-contrast lasers, which have recently become available [1,2] and used successively in laser-nanometer foil interaction experiments [27].

This work was supported by the 973 Program (Project No. 2006CB806004), the Program of Shanghai Subject Chief Scientist (09XD1404300), and the National Natural Science Foundation of China (Project Nos. 10675155, 10834008, 60921004, and 10835003).

*Author to whom correspondence should be addressed: bfshen@mail.shcnc.ac.cn

[1] T. Wittmann *et al.*, Rev. Sci. Instrum. **77**, 083109 (2006).
[2] A. Jullien *et al.*, Opt. Lett. **30**, 920 (2005); V. Chvykov *et al.*, Opt. Lett. **31**, 1456 (2006); D. Homoelle *et al.*, Opt. Lett. **27**, 1646 (2002); R. Shah *et al.*, Opt. Lett. **34**, 2273 (2009).
[3] A. Pukhov, Phys. Rev. Lett. **86**, 3562 (2001).
[4] P. Mora, Phys. Rev. Lett. **90**, 185002 (2003).
[5] H. Schwoerer *et al.*, Nature (London) **439**, 445 (2006).
[6] B. M. Hegelich *et al.*, Nature (London) **439**, 441 (2006).
[7] L. O. Silva *et al.*, Phys. Rev. Lett. **92**, 015002 (2004).
[8] A. Macchi *et al.*, Phys. Rev. Lett. **94**, 165003 (2005).
[9] X. Zhang *et al.*, Phys. Plasmas **14**, 073101 (2007).
[10] B. Shen *et al.*, Phys. Rev. E **64**, 056406 (2001).
[11] T. Esirkepov *et al.*, Phys. Rev. Lett. **92**, 175003 (2004).
[12] X. Q. Yan *et al.*, Phys. Rev. Lett. **100**, 135003 (2008).
[13] T. Zh. Esirkepov *et al.*, Phys. Rev. Lett. **89**, 175003 (2002).
[14] L. Yin *et al.*, Laser Part. Beams **24**, 291 (2006).
[15] L. Ji *et al.*, Phys. Rev. Lett. **101**, 164802 (2008).
[16] T. Zh. Esirkepov *et al.* arXiv:0812.0401.
[17] B. Shen *et al.*, Phys. Rev. Lett. **89**, 275004 (2002).
[18] T. Brabec and F. Krausz, Rev. Mod. Phys. **72**, 545 (2000).
[19] A. Pukhov *et al.*, Appl. Phys. B **74**, 355 (2002).
[20] K. Schmid *et al.*, Phys. Rev. Lett. **102**, 124801 (2009).
[21] F. Tavella *et al.*, Opt. Lett. **32**, 2227 (2007).
[22] H. C. Wu *et al.*, Phys. Plasmas **12**, 113103 (2005); H. C. Wu *et al.*, Appl. Phys. Lett. **87**, 201502 (2005); H. C. Wu *et al.*, Laser Part. Beams **23**, 417 (2005).
[23] R. Lichters, R. E. W. Pfund, and J. Meyer-ter-Vehn, LPIC++, Max-Planck-Institut für Quantenoptik Report No. MPQ225, Garching, Germanny, 1997.
[24] B. Shen *et al.*, Phys. Plasmas **8**, 1003 (2001).
[25] C. S. Lai, Phys. Rev. Lett. **36**, 966 (1976).
[26] G. Mourou *et al.*, Plasma Phys. Rep. **28**, 12 (2002).
[27] A. Henig *et al.*, Phys. Rev. Lett. **103**, 045002 (2009).